

# **Nonlinear Radial Consolidation Analysis of Vertical Drains Foundation under Cyclic Loadings**

**Abstract:** Aiming at the stability of storage facilities built in soft soil areas, this paper analyzes the influence of cyclic loading on consolidation during used stage. Firstly, the nonlinear compressibility and permeability of soil are introduced, the well resistance and three kinds of radial permeability coefficient modes are considered, the corresponding governing equations are obtained, and the corresponding analytical solution is obtained by the separate variables method. Then, the corresponding solution under the action of trapezoidal and triangular cyclic loading is obtained. The rationality of the solution in this paper is verified by the degradation method. Finally, the settlement of storage facilities during the using period is predicted by case analysis. The results show that the ratio of soil compression index to permeability index ( $C_c/C_k$ ) and the radial permeability coefficient mode have no significant influence on the average consolidation degree. The load-related intermittent parameter  $\beta$ , the loading parameter  $\alpha$ , and the parameter  $N_\sigma$  have a great influence on the average consolidation degree. The smaller the three parameters are, the more energy the load generates at the same time, and the greater the corresponding average degree of consolidation. **The solution can be effectively applied to nonlinear radial consolidation analysis under trapezoidal and triangular cyclic loadings.**

**Keywords:** consolidation, nonlinearity, vertical drain foundation, well resistance, cyclic loading

## **1、INTRODUCTION**

Many storage facilities have been built in the soft soil areas of various countries for storing food, oil, and liquefied natural gas resources. Storage facilities often bear repeated loads and unloaded in the use stage, which could be regarded as low-frequency cyclic loading [1]. It is necessary to discuss the consolidation behavior of the foundation under these circumstances.

Baligh and Levadoux [2] and Juran and Bernardet [3] simulated cyclic loading in the consolidometer and tested that the excess pore water pressure cannot be completely dissipated under cyclic loading. Then, Favaretti and Soranzo [4,5] applied the above test methods to the actual working conditions to predict the silo settlement under triangular cyclic loading. Subsequently, Rahal and Vuez [6-8] pointed out that in the use of silos, the upper loading was not a dynamic loading, and it could be approximated as a sinusoidal cyclic loading. By comparing the measured settlement measurement results with the theoretical value, it was found that the two had a good consistency. Xie et al. [9] considered the nonlinear change of soil compressibility and obtained the one-dimensional nonlinear consolidation solution of single-layer soil foundation under trapezoidal cyclic loading. Razouki et al. [10,11] got the one-dimensional consolidation differential equation under haversine cyclic loading and proved that the number of cycles required for the average degree of consolidation to reach a stable state increased with the decrease of the dimensionless time factor, and the number of cycles required for the average degree of consolidation to reach a stable state increment with the increased frequency, and the increment of drainage plate spacing also slows down the consolidation process.

Indraratna et al. [12,13] used cyclic triaxial test to study the effectiveness of prefabricated vertical drains in improving the stability of soft soil under cyclic loading, and the results showed that the excess pore water pressure generated during cyclic loading could be effectively reduced under drainage conditions. Mütting et al. [14] pointed out that the decrease of loading function frequency leads to the increase of the maximum effective stress and converges to a steady state after several cycles. Xu et al. [15] demonstrated that the larger loading cyclic period led to a larger amplitude of effective stress oscillation. The consolidation parameters related to the depth of soil mostly affect the amplitude of effective stress oscillation. Kim et al. [16,17] derived the analytical solution of foundation consolidation under cyclic loading considering the nonlinear compressibility and permeability of soil. Jiang et al. [18] considered the nonlinear compressibility and permeability of soil, deduced the nonlinear consolidation control equation considering the variation of permeability coefficient and well resistance in smearing area under instantaneous loading, and obtained the solution of the control equation. Zhu et al. [19] obtained that under cyclic loading, the average degree of consolidation presented a cyclic state, and gradually entered a stable cyclic state with the increase in cycles. Hu [20] pointed out that the pore water pressure and average consolidation degree in the soil are greatly affected by the loading form and loading period. Amiri [21] obtained through the test that the final settlement of the specimen would increase with the shortening of the loading and unloading process of the cyclic loading.

At present, scholars have done a lot of research on the consolidation of soft soil foundation under cyclic loading, but there is little consideration on the consolidation of shaft foundation under cyclic loading. It can be seen from the above literature that under cyclic loading, the average consolidation degree presents a cyclic state, and gradually enters a stable cyclic state with time. Based on the actual engineering background, the loading in the use of storage facilities is regarded as a low-frequency cyclic loading with constant loading. The nonlinear compressibility and permeability of soil are introduced, and the well resistance and three radial permeability coefficients are considered. The corresponding solutions are obtained and the effects of different parameters on consolidation are analyzed.

## 2、 BASIC ASSUMPTIONS, OBJECTIVES, EQUATIONS, AND SOLUTIONS

In Figure 1, the radial permeability coefficient of the smear zone and the undisturbed zone is defined as  $k_r(r)$ ,  $r$  and  $z$  represent radial and vertical coordinates respectively.  $q$  denotes the cyclic loading varied with time. The calculated thickness is  $H$ . The vertical permeability coefficient of soil is  $k_v$ . The corresponding permeability coefficients of the vertical drain, smear zone and unsmear zone are  $k_w$ ,  $k_s$  and  $k_h$ , and the corresponding radii are  $r_w$ ,  $r_s$  and  $r_e$ .

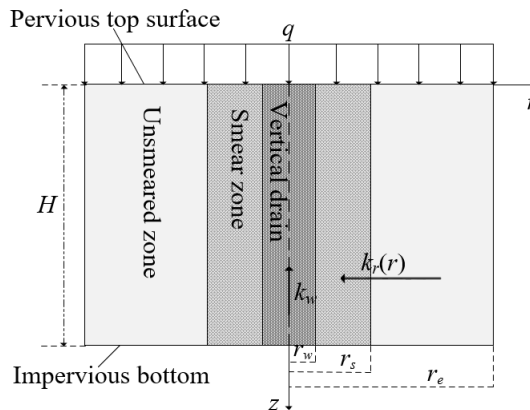


Fig.1 Calculation model for vertical drain

### 2.1 DERIVATION OF CONSOLIDATION EQUATION

According to the derivation process, the following assumptions are listed: (1) the equal strain assumption is established, the loading and settlement occur only in the vertical direction, and there is no lateral deformation in the shaft foundation, and the vertical deformation at any depth is the same; (2) Only radial flow of soil is considered, and flow in soil and vertical drain conforms to Darcy's law; (3) Except for the permeability coefficient, the other properties of the soil in the shaft and smearing area are the same as those in the undisturbed area; (4) Assuming that the loading is applied instantaneously; (5) At any depth, the amount of water flowing from the soil into the shaft is equal to the increment of water flowing upward in the shaft; (6) Considering the nonlinear changes of soil compressibility and permeability, the void ratio has the following relationship with effective stress and permeability coefficient :

$$e = e_0 - C_c \lg(\sigma'/\sigma'_0) \quad (1)$$

$$e = e_0 + C_k \lg(k_h/k_{h0}) \quad (2)$$

Where  $e$  and  $e_0$  are the void ratio at any time and the initial moment, respectively;  $\sigma'$  and  $\sigma'_0$  are the effective stress at any time and the initial effective stress, respectively;  $k_h$  and  $k_{h0}$  are the radial permeability coefficients of the soil at any time and the initial moment, respectively;  $C_c$  and  $C_k$  are the compression index and the permeability index, respectively.

Assuming that the radial permeability coefficient  $k_r(r)$  varies with the radial distance away from the vertical drain:

$$k_r(r) = k_h f(r) \quad (3)$$

where  $f(r)$  is the variation function of the permeability coefficient.

Based on the above assumptions, the radial consolidation control equation of vertical drain foundation [22]:

$$\frac{k_r(r)}{\gamma_w} \frac{1}{r} \frac{\partial}{\partial r} \left( r \frac{\partial u_r}{\partial r} \right) = - \frac{\partial \varepsilon_v}{\partial t}, r_w \leq r \leq r_e \quad (4)$$

According to assumption (5), the flow continuity equation is obtained :

$$2\pi r_w \frac{k_s}{\gamma_w} \frac{\partial u_r}{\partial r} \Big|_{r=r_w} = -\pi r_w^2 \frac{1}{\gamma_w} \frac{\partial}{\partial z} \left( k_w \frac{\partial u_w}{\partial z} \right) \quad (5)$$

Where  $u_w$  is the average excess pore water pressure in the vertical drain.

The expression of average excess pore water pressure is :

$$\bar{u}_r = \frac{1}{\pi (r_e^2 - r_w^2)} \int_{r_w}^{r_e} 2\pi r u_r dr \quad (6)$$

The boundary conditions are:

$$(1) \text{ Continuity of pore water pressure at } r = r_w, u_r = u_w \quad (7.1)$$

$$(2) \text{ Impermeable cylindrical surface at } r = r_e, \frac{\partial u_r}{\partial r} = 0 \quad (7.2)$$

$$(3) \text{ At the top of the clay layer } z = 0, u_w = 0 \quad (7.3)$$

---


$$(4) \text{ For the impervious bottom } z = H, \frac{\partial u_w}{\partial z} = 0 \quad (7.4)$$

$$(5) \text{ For the impervious bottom } t = 0, \bar{u}_r = q(t = 0) \quad (7.5)$$

Integrating both the left and right ends of Eq.(4) over  $r$  and using the boundary condition (7.2):

$$\frac{\partial u_r}{\partial r} = \frac{\gamma_w}{2k_h} \frac{1}{f(r)} \left( \frac{r_e^2}{r} - r \right) \frac{\partial \varepsilon_v}{\partial t} \quad (8)$$

Then integrating both the left and right ends of Eq.(8) simultaneously over  $r$  and using the boundary condition (7.1):

$$u_r = \frac{\gamma_w}{2k_h} \frac{1}{f(r)} \frac{\partial \varepsilon_v}{\partial t} [r_e^2 \bar{B}(r) - \bar{C}(r)] + u_w \quad (9)$$

$$\text{Where } \bar{B}(r) = \int_{r_w}^r \frac{1}{\xi f(\xi)} d\xi, \quad \bar{C}(r) = \int_{r_w}^r \frac{\xi}{f(\xi)} d\xi$$

Substitute Eq.(9) into Eq.(6), the average excess pore water pressure expression is obtained :

$$\bar{u}_r = \frac{\gamma_w r_e^2}{2k_h} F_c \frac{\partial \varepsilon_v}{\partial t} + u_w \quad (10)$$

$$\text{Where } F_c = \frac{2(r_e^2 \bar{\bar{B}} - \bar{\bar{C}})}{r_e^2 (r_e^2 - r_w^2)}, \quad \bar{\bar{B}} = \int_{r_w}^r r \bar{B}(r) dr, \quad \bar{\bar{C}} = \int_{r_w}^r r \bar{C}(r) dr.$$

When  $r=r_w$ ,  $k(r)=k_s$ . According to Eq.(8):

$$\left. \frac{\partial u_r}{\partial r} \right|_{r=r_w} = \frac{\gamma_w r_w}{2k_s} (n^2 - 1) \frac{\partial \varepsilon_v}{\partial t} \quad (11)$$

Substitute Eq.(11) into Eq.(5):

$$\frac{\partial^2 u_w}{\partial z^2} = -\frac{\gamma_w}{k_w} (n^2 - 1) \frac{\partial \varepsilon_v}{\partial t} \quad (12)$$

$$\text{Where } \frac{\partial \varepsilon_v}{\partial t} = m_v \frac{\partial \sigma'}{\partial t} = m_v \frac{\partial \sigma'}{\partial T_h} \frac{\partial T_h}{\partial t} = \frac{k_{h0}}{4r_e^2 \gamma_w} \frac{\sigma'_0}{\sigma'} \left( \frac{\partial q(T_h)}{\partial T_h} - \frac{\partial \bar{u}_r}{\partial T_h} \right) \quad (13)$$

In Eq.(13),  $m_v$  is defined as:

$$m_v = -\frac{1}{1+e_0} \frac{\partial e}{\partial \sigma'} = m_{v0} \left( \frac{\sigma'_0}{\sigma'} \right) \quad (14)$$

$$m_{v0} = \frac{C_c}{(1+e_0) \sigma'_0 \ln 10}$$

Substitute Eq.(13) into Eq.(10):

$$\frac{\partial \bar{u}_r}{\partial T_h} = \frac{\partial q}{\partial T_h} - \frac{8k_h}{F_c k_{h0}} \frac{\sigma'}{\sigma'_0} (\bar{u}_r - u_w) \quad (15)$$

Substitute Eq.(10) into Eq.(12):

$$\frac{\partial^2 u_w}{\partial z^2} = -\frac{2k_h(n^2-1)}{k_w r_e^2 F_c} (\bar{u}_r - u_w) \quad (16)$$

Substitute Eq.(1) into Eq.(15):

$$\frac{\partial \bar{u}_r}{\partial T_h} = \frac{\partial q}{\partial T_h} - \frac{8}{F_c} \left(\frac{\sigma'}{\sigma_0}\right)^{1-(C_c/C_k)} (\bar{u}_r - u_w) \quad (17)$$

Let  $\lambda = (8/F_c)(\sigma'/\sigma_0)^{1-(C_c/C_k)}$ , Then Eq.(17) becomes,

$$\frac{\partial \bar{u}_r}{\partial T_h} = \frac{\partial q}{\partial T_h} - \lambda (\bar{u}_r - u_w) \quad (18)$$

Substitute Eq.(1) into Eq.(16):

$$\frac{\partial^2 u_w}{\partial z^2} = -\frac{2k_{h0}(n^2-1)}{k_w r_e^2 F_c} \left(\frac{\sigma'}{\sigma_0}\right)^{-(C_c/C_k)} (\bar{u}_r - u_w) \quad (19)$$

Let  $\rho = (2k_{h0}(n^2-1)/k_w r_e^2 F_c)(\sigma'/\sigma_0)^{-(C_c/C_k)}$ , Then Eq.(19) becomes:

$$\frac{\partial^2 u_w}{\partial z^2} = -\rho (\bar{u}_r - u_w) \quad (20)$$

According to the principle of effective stress  $\sigma' = \sigma'_0 + q - \bar{u}_r$ , Then  $\sigma'$  is changed from initial  $\sigma'_0$  to final  $\sigma'_0 + q_u$ , Then taking the average value  $\frac{\sigma'_0 + \sigma'_0 + q_u}{2}$  as the value of  $\sigma'$  for solved, Let

$N_\sigma = (\sigma'_0 + q_u)/\sigma'_0$ , then the corresponding  $\lambda$  and  $\rho$  are become :

$$\lambda = \lambda' = \frac{8}{F_c} \left(\frac{1+N_\sigma}{2}\right)^{1-\frac{C_c}{C_k}} \quad (21)$$

$$\rho = \rho' = \frac{2k_{h0}(n^2-1)}{k_w r_e^2 F_c} \left(\frac{1+N_\sigma}{2}\right)^{\frac{C_c}{C_k}}$$

From Eq.(18), Eq.(20) and Eq.(21):

$$\frac{\partial^3 u_w}{\partial z^2 \partial T_h} + \lambda' \frac{\partial^2 u_w}{\partial z^2} - \rho' \frac{\partial u_w}{\partial T_h} = -\rho' \frac{\partial q}{\partial T_h} \quad (22)$$

Applying the separation of variables method to Eq.(22), the general solution is assumed to be

$$u_w = \sum_{m=1}^{\infty} T_m(T) \sin\left(\frac{M}{H} z\right) \quad (23)$$

Where  $M = \frac{2m-1}{2} \pi$ , ( $m=1,2,3,\dots$ ).

From Eq.(23) and Eq.(20), the expression of average excess pore water pressure is :

$$\bar{u}_r = u_w - \frac{1}{\rho'} \frac{\partial^2 u_w}{\partial z^2} \quad (24)$$

Combined with boundary conditions (7.3), (7.4) and (7.5) and Eq.(22), the solution of Eq.(24) is :

$$\bar{u}_r = \sum_{m=1}^{\infty} \frac{2}{M} e^{-\beta_m T_h} \sin\left(\frac{M}{H} z\right) \left( q(0) + \int_0^{T_h} \frac{dq}{d\tau} e^{\beta_m \tau} d\tau \right) \quad (25)$$

Where  $\beta_m = \left( \lambda' \left( \frac{M}{H} \right)^2 \right) / \left( \rho' + \left( \frac{M}{H} \right)^2 \right)$ .

To consider the influence of vertical drain construction on the permeability coefficient of the surrounding soil, according to reference [23], three various modes of radial permeability coefficient are selected, as shown in Fig. 2:

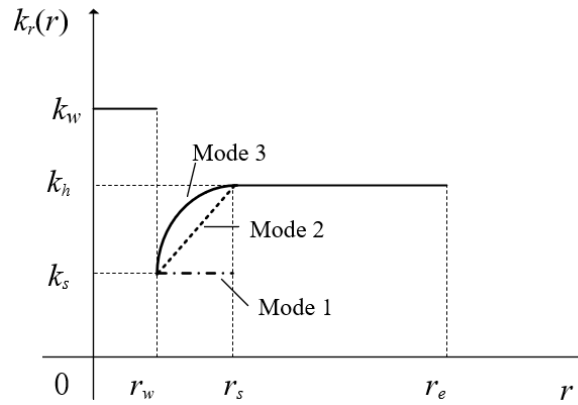


**Fig.2 Three variation modes of radial permeability coefficient in the smear zone**

Mode 1 shows that the radial permeability coefficient is  $k_s$  in the smear zone  $r_w \leq r \leq r_s$ , and  $k_h$  in the unsmeared zone  $r_s \leq r \leq r_e$ . The corresponding  $f(r)$  and parameter  $F_c$  are :

$$f(r) = \begin{cases} 1, & r_w, r, r_s \\ \alpha, & r_s < r, r_e \end{cases} \quad (26)$$

$$F_c = \left( \ln \frac{n}{s} + \alpha \ln s - \frac{3}{4} \right) \frac{n^2}{n^2 - 1} + \frac{s^2}{n^2 - 1} (1 - \alpha) \times \left( 1 - \frac{s^2}{4n^2} \right) + \alpha \frac{1}{n^2 - 1} \left( 1 - \frac{1}{4n^2} \right) \quad (27)$$

Where  $\alpha = k_h/k_s > 1$ .

Mode 2 shows that the radial permeability coefficient of the soil in the smear zone decreases gradually to  $k_s$  with the decrease of  $r$ , and the radial permeability coefficient of the unsmeared zone is  $k_h$ . This mode is more realistic than mode 1, and the corresponding  $f(r)$  and parameter  $F_c$  are :

$$f(r) = \begin{cases} \frac{r - r_w}{r_s - r_w} (1 - \alpha) + \alpha, & r_w, r, r_s \\ 1, & r_s < r, r_e \end{cases} \quad (28)$$

$$F_c = \frac{n^2}{n^2-1} \left\{ \frac{s-1}{\alpha s-1} \ln(\alpha s) - \frac{(s-1)^2}{n^2(1-\alpha)} + \frac{2(s-1)(\alpha s-1)}{n^2(1-\alpha)^2} \ln \frac{1}{\alpha} - \frac{2(s-1)}{n^4(1-\alpha)} \left( \frac{s^3-1}{3} - \frac{s^2-1}{2} \right) \right. \\ \left. - \frac{(s-1)(\alpha s-1)}{n^4(1-\alpha)^2} \left[ \frac{s^2-1}{2} - \frac{(s-1)(\alpha s-1)}{(1-\alpha)} + \frac{(\alpha s-1)^2}{(1-\alpha)^2} \ln \frac{1}{\alpha} \right] - \frac{(n^2-s^2)(1-s)^2}{n^4(1-\alpha)} + \ln \frac{n}{s} - \frac{3}{4} + \frac{4n^2s^2-s^4}{4n^4} \right\} \quad (29)$$

Mode 3 shows that the radial permeability coefficient of soil in the smear zone presents a parabolic change with the increase of  $r$ , which increases from  $k_s$  to  $k_n$ . The radial permeability coefficient of soil in the unsmeared zone remains unchanged. This mode is the change of permeability coefficient measured by Indraratna et al. [24,25], and the corresponding  $f(r)$  and parameter  $F_c$  are :

$$f(r) = \begin{cases} (1-\alpha) \left( a - b + c \frac{r}{r_w} \right) \left( a + b - c \frac{r}{r_w} \right), & r_w, r, r_s \\ 1, & r_s < r, r_e \end{cases} \quad (30)$$

Where  $a = \sqrt{1/(1-\alpha)}$ ,  $b = s/(s-1)$ ,  $c = 1/(s-1)$ ,  $d = \ln[(a+1)/(a-1)]$ .

$$F_c = (a^2 F_{c1} + n^2 F_{c2}) / (n^2 - 1) \quad (31)$$

Where

$$F_{c1} = \frac{1}{a^2 - b^2} \left( s^2 \ln s - \frac{s^2}{2} + \frac{1}{2} \right) - \frac{1}{(a^2 - b^2)c^2} \left[ -b + \frac{1}{2} + \left( \frac{a^2}{2} - b^2 \right) \ln \alpha + \frac{abd}{2} \right] \\ + \frac{1}{n^2 c^4} \left[ -3b + \frac{1}{2} + \left( \frac{a^2}{2} + b^2 \right) \ln \alpha + \frac{3abd}{2} \right] \quad (32)$$

$$F_{c2} = \ln \frac{n}{s} - \frac{3}{4} + \frac{s^2}{n^2} - \frac{s^4}{4n^4} + a^2 \left( 1 - \frac{s^2}{n^2} \right) \left[ \frac{1}{(a^2 - b^2)} \left( \ln(s\sqrt{\alpha}) - \frac{bd}{2a} \right) - \frac{1}{n^2 c^2} \left( \ln \sqrt{\alpha} + \frac{bd}{2a} \right) \right]$$

The self-weight of storage facilities has always existed during eachstage. In this paper, the trapezoidal and triangular cyclic loading modes with constant loads are selected (shown in Fig.3 ). Each cycle of the cyclic load is  $t_0$ ,  $N$  is a positive integer starting from 1, indicating the number of cycles,  $\alpha$  is the loading parameter, and the time of loading and unloading is  $\alpha t_0$ . If  $\alpha = 0.5$ , the trapezoidal cyclic loading becomes a triangular cyclic loading, and  $\beta$  represents the interval of the loading:

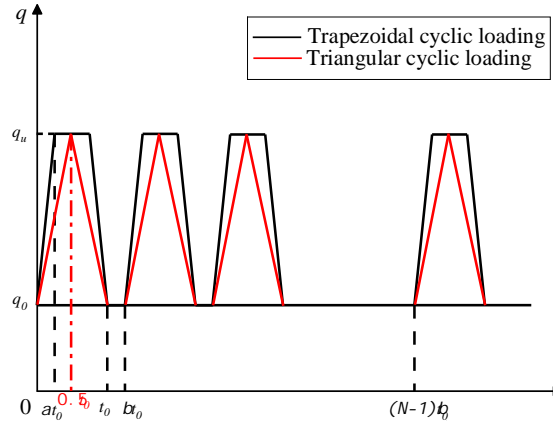


Fig.3 Schematic diagram of Trapezoidal and Triangular cyclic loadings

Defining dimensionless parameters:  $T_a = \frac{C_{h0}(N-1)\beta t_0}{4r_e^2}$ ,  $T_d = \frac{C_{h0}\alpha t_0}{4r_e^2}$ ,  $T_b = \frac{C_{h0}((N-1)\beta + 1)t_0}{4r_e^2}$ ,

$$T_h = \frac{C_{h0}t}{4r_e^2}.$$

The expression of loading  $q$  is :

$$q = \begin{cases} \frac{q_u - q_0}{T_d}(T_h - T_a) + q_0, & T_a \leq T_h \leq T_a + T_d \\ q_u, & T_a + T_d \leq T_h \leq T_b - T_d \\ -\frac{(q_u - q_0)}{T_d}(T_h - T_b) + \alpha q_0, & T_b - T_d \leq T_h \leq T_b \\ q_0, & T_b \leq T_h \leq T_a \end{cases} \quad (33)$$

Substitute Eq.(33) into Eq.(25) to obtain the expression of average excess pore water pressure:

$$\bar{u}_r = \begin{cases} \sum_{m=1}^{\infty} \frac{2}{M} \exp(-\beta_m T_h) [q_0 + T_1] \sin\left(\frac{M}{H} z\right), & T_a \leq T_h \leq T_a + T_d \\ \sum_{m=1}^{\infty} \frac{2}{M} \exp(-\beta_m T_h) [q_0 + T_2] \sin\left(\frac{M}{H} z\right), & T_a + T_d \leq T_h \leq T_b - T_d \\ \sum_{m=1}^{\infty} \frac{2}{M} \exp(-\beta_m T_h) [q_0 + T_3] \sin\left(\frac{M}{H} z\right), & T_b - T_d \leq T_h \leq T_b \\ \sum_{m=1}^{\infty} \frac{2}{M} \exp(-\beta_m T_h) [q_0 + T_4] \sin\left(\frac{M}{H} z\right), & T_b \leq T_h \leq T_a \end{cases} \quad (34)$$

Where

$$\begin{aligned} T_1 &= \frac{q_u - q_0}{\beta_m T_d} [D_T(N-1) + D_{T1}], T_2 = \frac{q_u - q_0}{\beta_m T_d} [D_T(N-1) + D_{T2}], \\ T_3 &= \frac{q_u - q_0}{\beta_m T_d} [D_T(N-1) + D_{T2} - D_{T3}], T_4 = \frac{q_u - q_0}{\beta_m T_d} [D_T(N)], \\ D_T &= \sum_{N=1}^n (D_{T2} - D_{T4}), D_{T1} = \exp(\beta_m T_h) - \exp(\beta_m T_a), \\ D_{T2} &= \exp(\beta_m (T_a + T_d)) - \exp(\beta_m T_a), D_{T3} = \exp(\beta_m T_h) - \exp(\beta_m (T_b - T_d)), \\ D_{T4} &= \exp(\beta_m T_b) - \exp(\beta_m (T_b - T_d)). \end{aligned} \quad (35)$$

The average consolidation degree  $U_p$  defined by excess pore water pressure is :

$$U_p = \left( \int_0^H (q - \bar{u}_r) dz / \int_0^H q_u dz \right) \quad (36)$$

The average consolidation degree  $U_s$  defined by deformation is :

$$U_s = \left( \int_0^H \varepsilon dz / \int_0^H \varepsilon_f dz \right) \quad (37)$$

Where  $\varepsilon = \frac{e_0 - e}{1 + e_0} = \frac{c_c}{1 + e_0} \log\left(\frac{\sigma'}{\sigma'_0}\right)$  is the vertical strain at any time,  $\varepsilon_f = \frac{e_f - e}{1 + e_0} = \frac{c_c}{1 + e_0} \log\left(\frac{\sigma'_f}{\sigma'_0}\right)$  is

the vertical strain at any time,  $\sigma'_f$  is the final effective stress.

## 2.2 DEGRADATION VERIFICATION

Reference [18] gave the expression of average excess pore water pressure of vertical drain foundation considering the change of well resistance with time :

$$\bar{u}_r = \sum_{m=1}^{\infty} \frac{2q_u}{M} \sin\left(\frac{Mz}{H}\right) \left(\frac{1+F_t}{1+F_0}\right)^{\lambda_a/\omega} \quad (38)$$

Where  $F_t = F_0 \exp(-\omega t)$ ,  $F_0 = M^2 / (\rho_a H^2)$ , conditions for constant well resistance at  $\omega = 0$  :

$$\lim_{\omega \rightarrow 0} \left(\frac{1+F_t}{1+F_0}\right)^{\lambda_a/\omega} = \exp\left(-\frac{\lambda_a M^2}{\rho_a H^2 + M^2} t\right) \quad (39)$$

Substitute Eq.(39) into Eq.(38) to obtain:

$$\bar{u}_r = \sum_{m=1}^{\infty} \frac{2q_u}{M} \sin\left(\frac{M}{H} z\right) \exp\left(-\frac{\lambda_a M^2}{\rho_a H^2 + M^2} t\right) \quad (40)$$

The expression of average excess pore water pressure is :

$$\bar{u}_r = \sum_{m=1}^{\infty} e^{-\beta_m T_h} \sin\left(\frac{M}{H} z\right) \frac{2}{M} (q(0) + \int_0^{T_h} \frac{dq}{d\tau} e^{\beta_m \tau} d\tau) \quad (25)$$

Where  $\beta_m = (\lambda'(\frac{M}{H})^2) / (\rho' + (\frac{M}{H})^2)$ . The loading on the right side of Eq.(25) changed with time is

regarded as a constant loading  $q_u$ , get  $\partial q / \partial T_h = 0$ , substitute  $\beta_m$  into Eq.(25) to obtain :

$$\bar{u}_r = \sum_{m=1}^{\infty} \frac{2q_u}{M} \sin\left(\frac{M}{H} z\right) \exp\left(-\frac{\lambda' M^2}{\rho' H^2 + M^2} T_h\right) \quad (41)$$

It can be seen that Eq.(41) is consistent with Eq.(40). By studying the degradation of the solution and comparing it with the existing analytical solution, the rationality of the solution is verified.

## 3、CONSOLIDATION BEHAVIOR UNDER CYCLIC LOADINGS

This paper mainly demonstrates the influence of  $C_d/C_k$ , different radial permeability coefficient modes, loading parameters  $\alpha$ , intermittent parameters  $\beta$ , and  $N_\sigma$  on consolidation. According to reference [24], the loading parameter  $\alpha$  of trapezoidal cyclic loading is 0.2, the interval parameter  $\beta$  of trapezoidal and triangular cyclic loadings is 1.2, and the calculated parameter is  $\sigma'_0=50$  kPa,  $q_u=75$  kPa,  $q_0=40$  kPa,  $C_d/C_k=1.5$ ,  $r_d/r_w=15$ ,  $r_s/r_w=4$ ,  $k_f/k_s=5$ ,  $k_w/k_{r0}=5000$ .

### 3.1 THE INFLUENCE OF $C_d/C_k$ ON CONSOLIDATION

Figure 4 is the average consolidation curve corresponding to different  $C_d/C_k$  values under trapezoidal and triangular cyclic loadings. It shows that with the increase of  $C_d/C_k$  value, the time to reach the stable state under the same type of cyclic loading is prolonged, that is, the consolidation rate is reduced. Under different

$C_d/C_k$  values,  $U_{s1}$  is higher than the corresponding  $U_p$ , indicating that the deformation rate is faster than the dissipation rate of pore pressure in the consolidation process. At the same time, the energy generated by trapezoidal cyclic loading is more than that generated by triangular cyclic loading, resulting in a larger average degree of consolidation corresponding to trapezoidal cyclic loading.

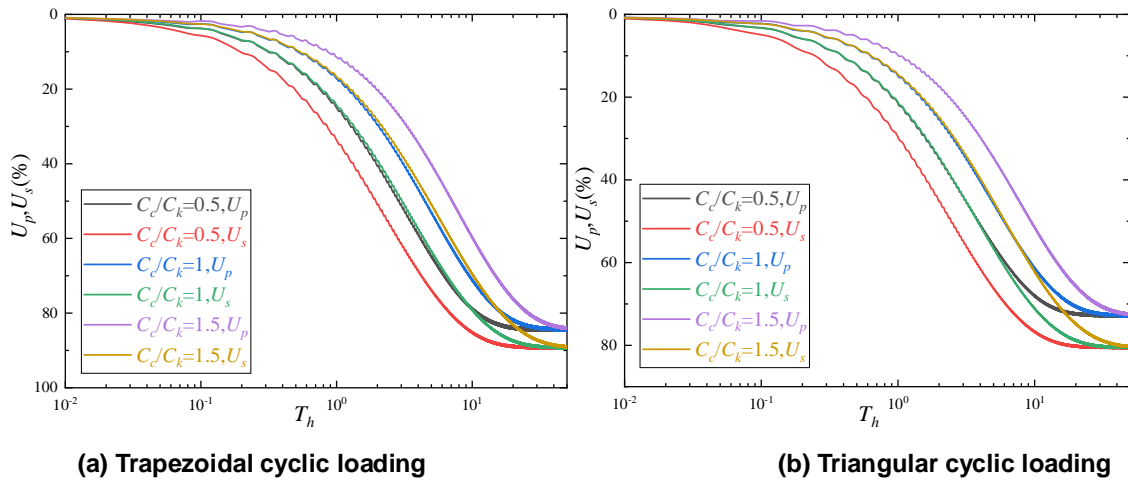


Fig.4 Average degree of consolidation at different values of  $C_d/C_k$

### 3.2 THE INFLUENCE OF DIFFERENT MODES OF RADIAL PERMEABILITY COEFFICIENT ON CONSOLIDATION

Figure 5 shows the average consolidation curve of different radial permeability coefficient modes under trapezoidal and triangular cyclic loadings. From figure 2, it could be seen that the radial permeability coefficient corresponding to modes 2 and 3 in the smear zone is larger than those of mode 1, but the difference between the two is small, so there is little difference between the consolidation rate corresponding to mode 2 and 3, which is greater than the curve corresponding to mode 1.

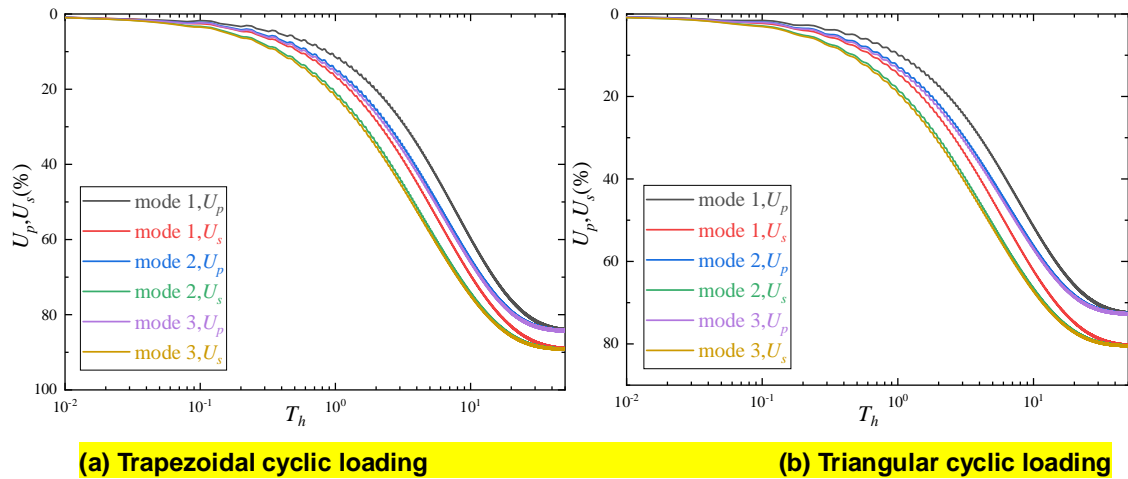


Fig.5 Average degree of consolidation corresponding to different modes of radial permeability coefficient

### 3.3 THE INFLUENCE OF INTERVAL PARAMETER $\beta$ AND THE LOADING PARAMETER $\alpha$ ON CONSOLIDATION

Figure 6 and Figure 7 respectively show the influence of the interval parameter  $\beta$  and the loading parameter  $\alpha$  on the average consolidation degree. Figure 6 shows that when the interval parameter  $\beta = 1$ , the

cyclic loading has no interval, and the corresponding average consolidation degree is the largest. With the increased  $\beta$ , the average consolidation degree gradually decreases. Figure 7 illustrates that the smaller the loading parameter  $\alpha$  is, the largest the average consolidation degree is. With the increased  $\alpha$ , the time when the loading is at the maximum  $q_u$  decreases, resulting in the decrease of the average consolidation degree. It implies that the smaller the parameter  $\beta$  is, the shorter the loading interval is, the smaller the parameter  $\alpha$  is, the faster the loading and unloading rate of the trapezoidal loading is, and the longer the duration of the constant loading is, the more the energy generated by the loading in the same time, resulting in the greater the average consolidation degree.

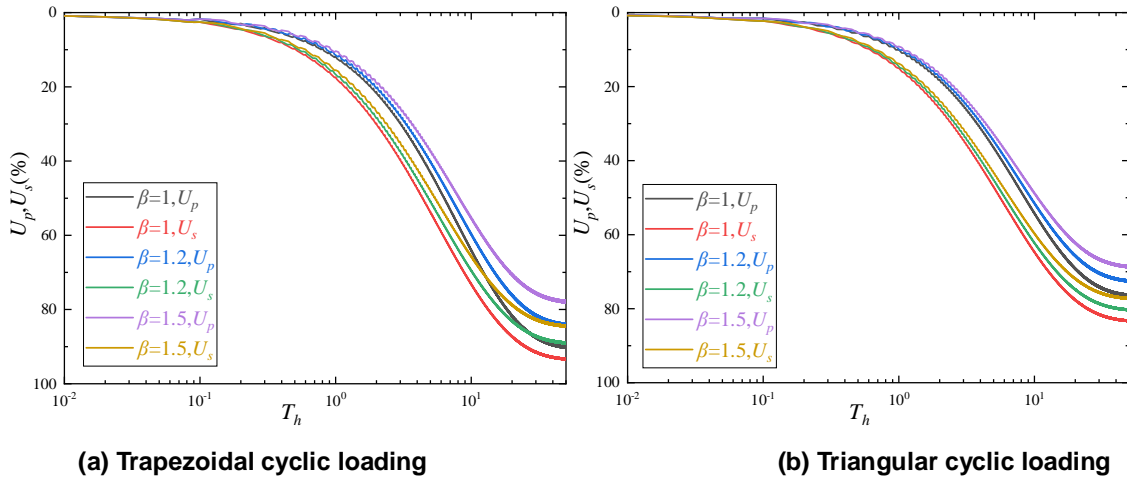


Fig.6 Effect of intermission parameter  $\beta$  on the average degree of consolidation

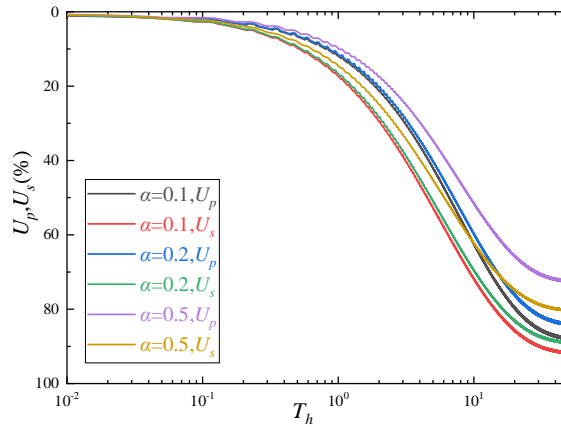


Fig.7 Effect of loading parameter  $\alpha$  on the average degree of consolidation under Trapezoidal cyclic loading

### 3.4 THE INFLUENCE OF $N_\sigma$ ON CONSOLIDATION

Figure 8 shows the average consolidation curves corresponding to different  $N_\sigma$  under trapezoidal and triangular cyclic loadings, respectively. Since the constant loading is considered in this paper, it can be seen that the smaller the  $N_\sigma$  is, the loading selected in this paper is closer to the constant loading, and the larger the corresponding average consolidation degree is.

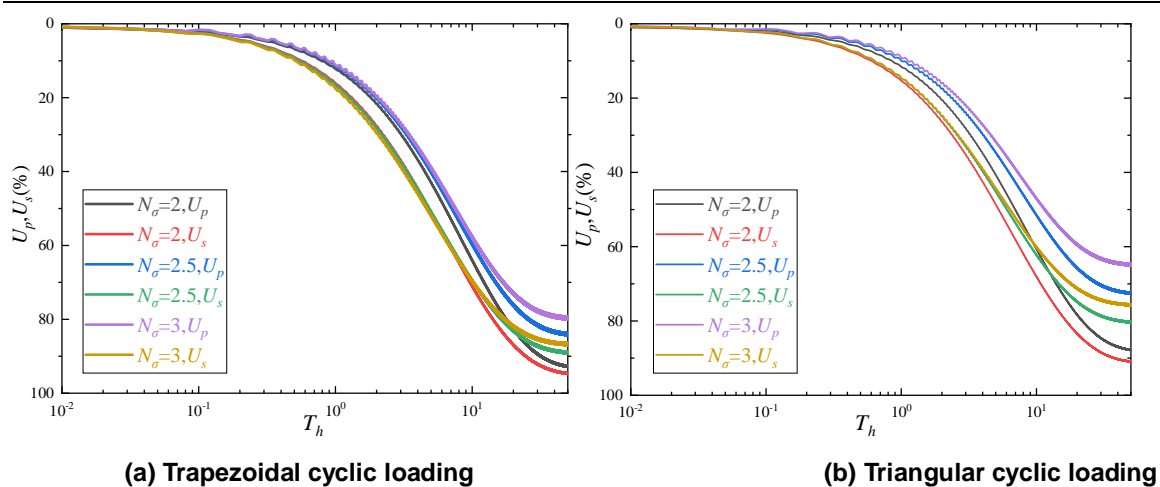


Fig.8 Average degree of consolidation at different values of  $N_\sigma$

#### 4. CASE ANALYSIS

A practical project built 10000 m<sup>3</sup> storage tank on a soft soil foundation in coastal areas. To reduce the settlement of the foundation, the prefabricated vertical drains were arranged in advance in the foundation, which can be regarded as the working condition of the upper part of the shaft foundation under cyclic loading in the use stage. In the use stage, the dimensionless loading time factor  $T_0$  is 17.46, the maximum loading is 165kPa, the intermittent period parameter  $\beta$  is 1.2, the loading parameter  $\alpha$  is 0.33, and the setting depth of prefabricated vertical drains is 20 m. Other parameters related to consolidation behavior is the same in this paper. The settlement curve of the tank within 2176 days ( $T_h=200$ ) is shown in Fig.9.

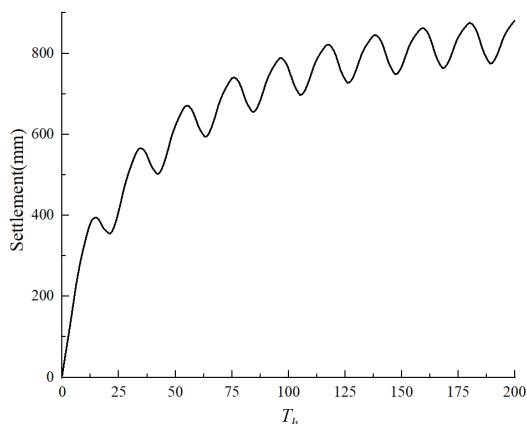


Fig.9 The method of this paper is used to predict the settlement of the use stage

The tank only carried out one-time water-filling preloading. It can be seen from Fig.9 that consolidation settlement still occurred in the early use stage, and the maximum settlement of the shaft foundation was about 767 mm. In the steady state of settlement, the maximum settlement difference due to loading and unloading is 86.34 mm, approximately 109 days ( $T_h=10$ ), and the daily settlement is about 0.8mm. The maximum settlement difference can be used as the designed reference to ensure the safety of later working condition.

#### 5 CONCLUSIONS

In this paper, the nonlinear consolidation solution of the vertical drain foundation considered constant well resistance and radial permeability coefficient variation under trapezoidal and triangular cyclic loadings is

---

derived. The accuracy and rationality of the solution are verified by degradation verification and case study, and the following conclusions are obtained:

(1) The analyses show that the average consolidation degree under cyclic loadings is lower than 100 %, indicating that the excess pore water pressure in the soil cannot be completely dissipated. The final value of the average consolidation degree is independent of the  $C_v/C_k$  value and the radial permeability coefficient mode, and these two parameters mainly affect the time when the average consolidation degree reaches a stable state. The smaller the  $C_v/C_k$  value, the shorter the time for the average degree of consolidation to reach a stable state, and the greater the radial permeability coefficient in the smear area, the faster the time for the average degree of consolidation to reach a stable state.

(2) Load-related parameters  $\beta$ ,  $\alpha$  and  $N_\sigma$  have a great influence on average consolidation degree. The smaller the intermission parameter  $\beta$  is, the shorter the intermission period of the load is, the more energy the load produces at the same time, which leads to the greater the average consolidation degree. The smaller the loading parameter  $\alpha$  is, the longer the trapezoidal cyclic load is in the  $q_u$  stage, the more the energy generated by the loading is, and the larger the corresponding average consolidation degree is. Since the loading method in this paper has constant loading, the smaller the  $N_\sigma$  is, the closer the loading form is to the constant load, and the larger the corresponding average consolidation degree is.

(3) For similar projects, it is necessary to estimate the loading parameters  $\beta$ ,  $\alpha$  and  $N_\sigma$  to avoid the safety hazard of the upper structure caused by the inaccuracy of parameter selection.

## REFERENCES

1. Zienkiewicz OC, Bettess P. Soils and other saturated media under transient, dynamic load conditions, Soil Mechanics-transient and Cyclic Loads, Pande and Zienkiewicz eds.: John Wiley and Sons, 1982.
2. Baligh MM, Levadoux JN. Consolidation theory for cyclic loading. Journal of the Geotechnical Engineering Division 1978;104(4):415-31.
3. Juran I, Bernardet A. La consolidation unidimensionnelle sous charge cyclique. Revue française de géotechnique 1986(36):17-30.
4. Favaretti M, Mazzucato A. Settlement of a silo subjected to cyclic loading. Vertical and Horizontal Deformations of Foundations and Embankments: ASCE, 1994:775-85.
5. Favaretti M, Soranzo M. A simplified consolidation theory in cyclic loading conditions. Compression and consolidation of clayey soils, 1995:405-9.
6. Rahal MA. Etude de la consolidation unidimensionnelle d'un kaolin soumis à des chargements par paliers et sinusoïdaux.: Rennes, INSA, 1993.
7. Vuez A, Rahal A. Cyclic loading for the measuring of soil consolidation parameters. Vertical and Horizontal Deformations of Foundations and Embankments: ASCE, 1994:760-74.
8. Rahal MA, Vuez AR. Analysis of settlement and pore pressure induced by cyclic loading of silo. J GEOTECH GEOENVIRON 1998;124(12):1208-10.
9. Xie K, Qi T, Dong Y. Nonlinear analytical solution for one-dimensional consolidation of soft soil under cyclic loading. J ZHEJIANG UNIV-SC A 2006;7(8):1358-64.
10. Razouki SS, Bonnier P, Datcheva M, Schanz T. Analytical solution for 1D consolidation under haversine cyclic loading. INT J NUMER ANAL MET 2013;37(14):2367-72.
11. Razouki SS. Radial consolidation clay behaviour under haversine cyclic load. Proceedings of the Institution of Civil Engineers-Ground Improvement 2016;169(2):143-9.

- 
12. Indraratna B, Attya A, Rujikiatkamjorn C. Experimental investigation on effectiveness of a vertical drain under cyclic loads. *J GEOTECH GEOENVIRON* 2009;135(6):835-9.
  13. Indraratna B, Ni J, Rujikiatkamjorn C. Investigation on effectiveness of a prefabricated vertical drain during cyclic loading. *IOP Conference Series: Materials Science and Engineering*: IOP Publishing, 2010:12091.
  14. MÜthing N, Razouki SS, Datcheva M, Schanz T. Rigorous solution for 1-D consolidation of a clay layer under haversine cyclic loading with rest period. *SpringerPlus* 2016;5(1):1-13.
  15. Xu C, Chen Q, Liang L, Fan X. Analysis of consolidation of a soil layer with depth-dependent parameters under time-dependent loadings. *EUR J ENVIRON CIV EN* 2018;22(sup1):s200-12.
  16. Kim P, Ri K, Kim Y, Sin K, Myong H, Paek C. Nonlinear consolidation analysis of a saturated clay layer with variable compressibility and permeability under various cyclic loadings. *INT J GEOMECH* 2020;20(8):4020111.
  17. Kim P, Kim H, Kim Y, Peak CH, Oh SN, So SR, et al. Nonlinear radial consolidation analysis of soft soil with vertical drains under cyclic loadings. *SHOCK VIB* 2020;2020:8810973.
  18. Wen-hao J, Liang-tong Z. Analytical solution for nonlinear consolidation of sand-drained ground with exponential flow under vacuum combined surcharge preloading. *Chinese Journal of Rock Mechanics and Engineering*. 2021;38(2):69-76.
  19. Zhu B, Shi G, Wei Z. One-Dimensional Nonlinear Consolidation Analysis Using Hansbo's Flow Model and Rebound-Recompression Characteristics of Soil under Cyclic Loading. *MATH PROBL ENG* 2021;2021:9919203.
  20. Hu J, Bian X, Chen Y. Nonlinear consolidation of multilayer soil under cyclic loadings. *EUR J ENVIRON CIV EN* 2021;25(6):1042-64.
  21. Amiri A, Toufigh MM, Toufigh V. An experimental investigation of the consolidation process under triangular cyclic loading. *P I CIVIL ENG-GEOTEC* 2020;173(2):125-32.
  22. Lu M, Wang S, Sloan SW, Indraratna B, Xie K. Nonlinear radial consolidation of vertical drains under a general time-variable loading. *INT J NUMER ANAL MET* 2015;39(1):51-62.
  23. Lu M, Wang S, Sloan SW, Sheng D, Xie K. Nonlinear consolidation of vertical drains with coupled radial-vertical flow considering well resistance. *GEOTEXT GEOMEMBRANES* 2015;43(2):182-9.
  24. Indraratna B, Perera D, Rujikiatkamjorn C, Kelly R. Soil disturbance analysis due to vertical drain installation. *P I CIVIL ENG-GEOTEC* 2015;168(3):236-46.
  25. Nguyen B, Kim Y. An analytical solution for consolidation of PVD-installed deposit considering nonlinear distribution of hydraulic conductivity and compressibility. *ENG COMPUTATION* 2019;36(2):707-730.